CHAPTER 5

COMPUTATIONAL ANALYSIS OF MODIFIED GEDUNIN COMPOUND $C_{26}H_{31}N_2O_6F$ AS A POTENTIAL INHIBITOR OF SNAKE VENOM ENZYMES

5.1. Introduction

According to WHO research, snakebites have become a widely ignored public health hazard, causing more than 137,880 fatalities in nations alone each year and poisoning almost two million people. Women, children, the poor, and farmers are particularly vulnerable, as medical resources are limited**(Gutiérrez *et al.*,2017).** Bites are fatal and include severe paralysis, irreversible kidney failure, permanent amputation of limbs, and disability. Patients with a snake bite in critical need immediate administration of an antidote. However, the antidote choice depends on the known species or is believed to be responsible for the bite. The first six hours after a bite are critical; hence, a specific antidote should be administered to protect the victim from toxic effects and death. The biggest challenge is the unavailability, underproduction, and storage of the expensive antidote currently available against large species, which is ineffective against lesser-known but widespread native species of snakes. Antiserum is life-saving; however, side effects such as serum sickness or delayed hypersensitivity cannot be neglected and have no reported effects in preventing local tissue damage due to the high levels of non-immunoglobulin proteins in the antiserum **(Devi *et al.*, 2002).** Alternatively, plant extracts have been effective against snake venom since ancient times and have attracted growing interest owing to their abundance and

safety **(Rajesh *et al.*, 2017).** A study suggested that plant species, for example, *Azadirachtaindica,* contain various compounds, such as steroids, alkaloids, triterpenoids, tetraterpenoids, tannins, phenols, pterocarpans, and glycosides. These are effective against snake venom by neutralizing multiple toxins and enzymes (hydrolases, proteases, phospholipase, ATPase, transaminase, and nucleotidase) **(Subapriya *et al.,* 2005).** Gedunin is a neem-tree-isolated tetranortriterpenoid used in traditional medical treatment for malaria and other infectious illnesses (*Azadirachta indica*, Meliaceae). Gedunin has also demonstrated an anti-proliferative action in several cancer cell lines, including prostate, colon, and ovarian malignancies. Gedunin is a powerful thiol-reactive electrophile that induces heat shock reactions. Help standard neem-reported agrochemical properties **(Subapriya et *al.,* 2005).** This study aimed to investigate the potential activity of the tetraterpenoid gedunin from ripened fruit extracts of neem (*Azadirachtaindica*) against snake venom enzymes, mainly 5'-nucleotidase, phospholipase, hydrolases, metalloproteinase, L-amino acid oxidase (L-aao), and Acetylcholinesterase. They are commonly found in all snake species.

Here computational analysis of modified gedunin compound $C_{26}H_{31}N_2O_6F$ as a potential inhibitor of snake venom enzymes focuses on the modification of gedunin in the poison enzyme active site pocket that led to gedunin derivative formation, which can act as an inhibitor $C_{26}H_{31}N_2O_6F$ against snake venom enzymes and also investigated its pharmacological properties.

5.2. Experimental

5.2.1. The ICM Method

ICM software was used to perform flexible ligand docking in the potential map grid calculated for the enzyme active site pocket.

The Monte Carlo method used in ICM follows a procedure **(Gutierrez *et al.*, 2017):** random movement in the conformational variable of the ligand in the enzyme pocket **(Devi *et al*., 2002).** Energy minimization of the complex **(Subapriya *et al.*, 2005)**. Calculating the desolvation energy was followed by selecting the minimized conformation using the Metropolis selection method, and the accepted lower energy conformation was the new calculated energy criterion. The thoroughness value, the user-defined multiplier, was kept at three according to the number of ligand rotational bonds. The pre-calculated grid maps for hydrogen bonds, vanderwaal bonds, and electrostatic and hydrophobic potentials reduced the time required for ligand sampling, and 0.5 Å grid distance maps were generated at the binding location. The global optimization of the energy carried out requires high dimensionality and is reduced in ICM by assigning internal coordinates to each atom **(Yamashita and Hashida, 2004).**

5.2.1.1 Ligand Preparation

The ligand was made by converting it into an ICM object by the depletion of water and optimization of hydrogen, his-pro-asn-gln-cys, carried out outside the pocket of the enzyme (receptor). The ligand is a modified form of gedunin called an inhibitor $C_{26}H_{31}N_2O_6F$. **(Figure 5.1) (Figure 5.2)**

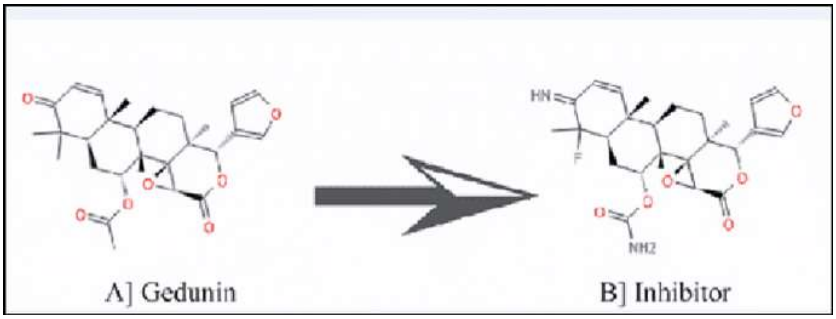

Figure 5.1. Gedunin was modified inside the venom enzyme pocket at 3 positions which include methyl substitution using ICM molsoft software.

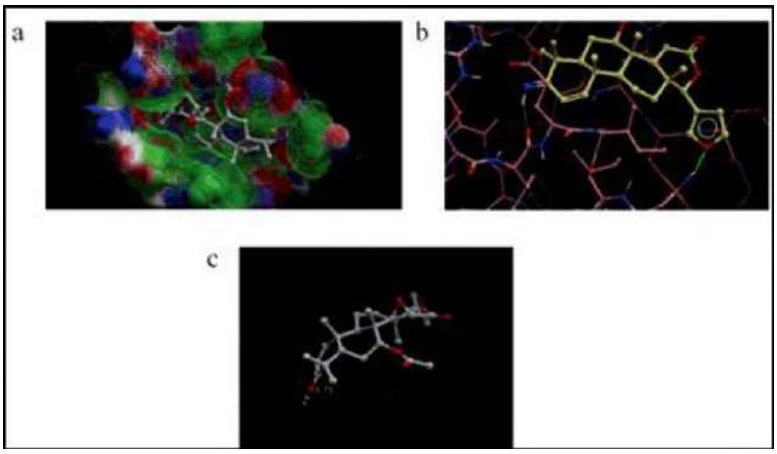

Figure 5.2 (a) Docked pose of inhibitor $C_{26}H_{31}N_2O_6F$ inside the active site of venom enzyme 5'Nucleotidase. (b) 3D view of the interaction between gedunin and neighbouring amino acids of 5'Nucleotidase. (c) 3D view of the change in the interaction between inhibitor $C_{26}H_{31}N_2O_6F$ and neighbouring amino acids of 5' Nucleotidase.

5.2.1.2.Receptor Preparation

The docking receptor file was downloaded from the RSCB PDBwith PDB ID: 5H7W, 3KVE,1ND1, 7M6C, 1FSS,5XRF, and receptors (snake venom enzymes) were produced by optimizing hydrogen and missing side chains, removing excess water bound to receptors, and converting the PDB coordinates to ICM internal coordinates in the ICM-Pro Molsoft- Software **(Pahler and Brink, 2013) (Smielewski *et al.*, *2012).***

5.2.1.3.Molecular Docking

ICM mol Soft Docking based on distorted probability Monte Carlo + local optimization and physically based scoring. A low ICM score and decrease in steric hindrance indicated a high probability of a binder. The binding energy is the sum of the steric and interaction energies between the ligand and receptor. The

lower the binding energy, the better the ligand**(Table- 5.1, 5.2, 5.3).** The inhibitor ($C_{26}H_{31}N_2O_6F$) was docked to snake venom enzymes: 5'nucleotidases, Acetylcholinesterase, L-aao, metalloproteinase, phospholipase A2, and thrombin-like hydrolase. Binding modes for poses that are ordered according to the score function prioritize the top poses. The predicted scores were the ICM and the potential mean force scores (PMF). The PMF score is based on structural knowledge of the receptor-ligand complex. In contrast, the ICM score is the sum of the ligand-target van der Waals interactions and the internal force field energy of the ligand (DE IntFF 5), hydrogen bond interactions (DE HBond Tor), conformational energy loss due to free energy change with ligand binding (TDS), ligand binding with solvation of electrostatic energy (DE HBDesol), hydrophobic free energy generation (DE HPhobSolEl), hydrogen bond interactions (DE HBond Tor), and hydrogen bridge acceptor-donor desolvation energy **(He *et al.,* 2016).**

Delta G = DEIntFF + TDS tor + þ a1DE HBond + þ a2 DEHBDesol + þ a3TE SolEI + þ a4TE EPhobe

Table 5.1 Binding energy of Inhibitor $C_{26}H_{31}N_2O_6F$ –Receptor enzyme complex.

Snake Venom Enzymes	Inhibitor $C_{26}H_{31}N_2O_6F$ Binding Energy (Kcal/mol)
5' Nucleotidase	-9.30
Acetylcholinesterase	-8.40
L – aao	-14.80
Metalloproteinase	-10.60
Phospholipase A2	-9.90
Thrombin like hydrolase	-9.60

Table 5.2. **HBond:-** Hydrogen Bond energy, **VwInt:-** The Vander Waals Interaction Energy (sum of van der waals), **Hphob:-** Hydrophobic Energy in

exposing a surface to the water, **N flex:-** Number of Rotatable torsions, **Eintl:-** Internal Conformational Energy of the ligand, **Dsolv:-** The desolvation of exposed H-bond donors and acceptors, **SolEl:-** The solvation electrostatics energy change upon binding, **Pmf Score:-**potential mean force score of ligand-receptor interaction strength. (Lower the score, better the strength), **DTSsc:** loss of entropy by the rotatable protein side-chains.

Enzyme name	Docked score	HBond	Hphob	VwInt	Eintl	Dsolv	SolEl	Pmf Score	DTSsc
Acetyl choline sterase	-14.98	-3.33	-3.63	-18.74	1.275	12.71	4.75	-51.33	0.93
5' Nucleotidase	-7.035	-1.748	-4.743	-19.32	1.61	17.32	7.156	-29.36	1.569
Metalloprotei nase	-9.993	-1.832	-4.864	-19.5	2.121	14.6	6.032	-85.76	1.083

Table 5.3. Illustration of Receptor pockets/ligand interaction site's pocket volume, area, Aromaticity, Hydrophobicity, and druggness probability. Buriedness of pocket ranges from 0 to 1 (open to wholly buried).

Enzyme	Pocket	Volume (m^3)	Area (m^2)	Hydrophobicity	Buriedness	Aromaticity	DLID prob*	Non-sphericity
Acetyl choline sterase	1	239.25	299.36	0.561896	0.739845	0.10058	0.03	1.606221
Metalloprotei nase	1	239.5	252.9	0.5673	0.745	0.1038	1	1.35
5' Nucleotidase	1	164.9	198.2	0.429	0.6769	0	0.71	1.363

Table 5.4. Depicting the physical properties of the Inhibitor $C_{26}H_{31}N_2O_6F$ molecule using ICM-Mol soft.

Molecular weight	486.2166 g/mol
HBA	9
HBD	3
RotB	3
Drug likeliness	-0.0341
Mol Area	466.626
Mol HF	-216.73
Mol half-life	1.62 years
Mol Log S	-5.09
Groups	Furan, Ester, Aldmine, Ether, Oxirane, Halo

5.2.2 Simulation

Gromacs used for MD (Molecular Dynamics) used the concept of a periodic boundary to create boxes/grids and groups to show the action in the OPLS force field for 50 ns **(Rawat *et al.,* 2021).**

5.2.3. Pharmacokinetics Analysis

As access to a physical sample is highly limited (Absorption, distribution, metabolism, excretion, and toxicity) ADMET is essential at the centre of the medical development process. These were predicted using the SwissADME too **(Figure 5.3.).**The HIA(human intestinal absorbtion) predicted a probability of 0.863636 for the modified inhibitor. P450 isoform classification was found to be 3A4 sites. Biostere and Derek Nexus probability properties of the inhibitor ($C_{26}H_{31}N_2O_6F$) were estimated using Star Drop Software **(Zou *et al.,* 2020)**, which is based on a probabilistic scoring algorithm. Derek Nexus is knowledge-based toxicology software that provides quantitative EC3 prediction. Plausible reports are seen in developmental toxicity, hepatotoxicity, and skin and eye

irritation. Toxicity prediction (LD50) was performed for oral administration using the web-based server, Protox-II.

5.3 Results and Discussion

The ligand is a modification of the gedunin compound, as shown in **Figure 5.1.** It was modified in the enzyme bag with the Ligand Edit function of ICM-Pro. The modification was selected after lowering the steric and the ICM score of gedunin, as shown in **Figure 5.2**. The modification resulted in increased hydrogen and non-covalent bonds with low steric hindrance, allowing easy binding of the inhibitor inside the pocket of the enzyme.

5.3.1 Molecular Docking

The results of the docking **(Daina *et al.*, 2017)** for the inhibitory compound investigated are given in **Table 5.1**. The L-aao (L-amino acid oxidase) enzyme-ligand complex has a binding energy of at least -14.80 kcal/mol binding energy, which indicates spontaneous binding of the inhibitor to the active substance of the enzyme L-aao and hence increased activity of the inhibitor in neutralizing the enzyme. The binding energy residues of the ligand enzyme complex were -9.30, -8.40, -10.60, -9.90, and -9.60 kcal/mol. It contains 5‟ nucleotidases, Acetylcholinesterase, metalloproteinase, phospholipase A2, and thrombin-like hydrolase enzymes. The inhibitor binds readily with metalloprotease enzymes, whereas there is an equal probability of binding with the rest of the enzymes. The inhibitor had the highest amount of petite binding in the case of AChE (Acetylcholinesterase). The binding energy is released when the receptor associates with the ligand. A negative value indicates that the interaction is spontaneous; therefore, a higher (-) value corresponds to better interaction.

The sum of the lattice score, electrostatic score, Hydrophobicity score, surface score, hydrogen bond score, van der waals interaction energy of ligand conformation and internal torsion, and interaction energy + lattice depict the ligand-free energy. The hydrogen bond score was calculated using the full receptor atom model and found to be -3.33, -1.748, and-1.832 for the three poses of inhibitor inside the pocket of the enzyme. The lowest score signifies the effective binding of the enzyme and inhibitor. The electrostatic score is calculated as the difference between the electrostatic interaction energy of the free ligand and the electrostatic interaction energy, which was found to be -18.74, -19.32, and - 19.5 for three poses of inhibitor inside the pocket of the enzyme. The lowest score signifies effective binding of the enzyme and inhibitor, with the Hp score calculated as the difference between the conformation of the free ligand and the hydrophobic interaction energy found as -3.63,-4.743, and-4.864 for Acetylcholinesterase, 5'nucleotidase, and metalloproteinase, respectively (**Table5.1)**. This implies that 5"nucleotidase and metalloproteinase have the least hydrophobic interactions with inhibitors. The PMF (potential mean force) score is a knowledge-based assessment of the structural information of enzyme-ligand complexes. **Table5.2** shows the evaluation function for ligand enzyme complexes based on intermolecular interactions and also shows energies such as hydrogen bond energy, the interactive energy of van der waals, the hydrophobic energy of water exposure, the number of rotating torsions, and the ligand's inner conformation energy. Solvation of exposed donors and acceptors of hydrogen bonds, shift in energy from electrostatic solvation to binding, and mean force value of ligand-receptor interaction strength **(Yamashita F and Hashida M, 2004).** Acetylcholinesterase had the least negative (preferred) ICM score of-14.98,

followed by -7.035, -9.993, and PMF score: of -51.33, followed by -29.36, -85.76 for 5‟nucleotidase or metalloproteinase, all with ICM scores <-15.0, and PMF scores <-37.5. 5'nucleotidase and metalloproteinase – inhibitor complex is less stable than Acetylcholinesterase –inhibitor complex. The selection of the enzyme docking sites based on the DLID likelihood of each pocket in the enzymes and buried pockets influences this drug score. The probability is highest in the active site of the enzyme. **Table 5.3** shows the DLID and pocket buridness of the enzymes. A pocket with a high DLID score is preferred because it has high drug-likeliness in enzymes which can be easily observed in molecular dynamics.

5.3.2 Simulation

Molecular dynamics is a method used to study the structure of compounds/solids using classical mechanics and to create a trajectory. Gromacs used for MD used the concept of a periodic boundary to create boxes/grids and groups to show the action. Simulation studies of 50 ns (nanosecond) show that the average angle between Gedunin and 5'NT enzyme is between 70-760, and density is between 980-984 kg/m3, which increased due to complex formation. The radius of gyration decreased from 1.2 to 1 after complex formation, implying the tight bonding of the complex. The number of hydrogen bonds between peptide-water is a maximum of 100-160; between peptide-peptide, their number is five. This indicates better and stronger binding between the enzyme and the inhibitor. The binding energies decreased considerably to ~ 0 Ki/mol, indicating structural stability. Initially, RMSD fluctuated from 2 nm to 8 nm, whereas after complex formation, RMSD became stable within 35ns, indicating complex formation. The pressure was approximately 400 bar, and the RMS was between 0.2-0.7.

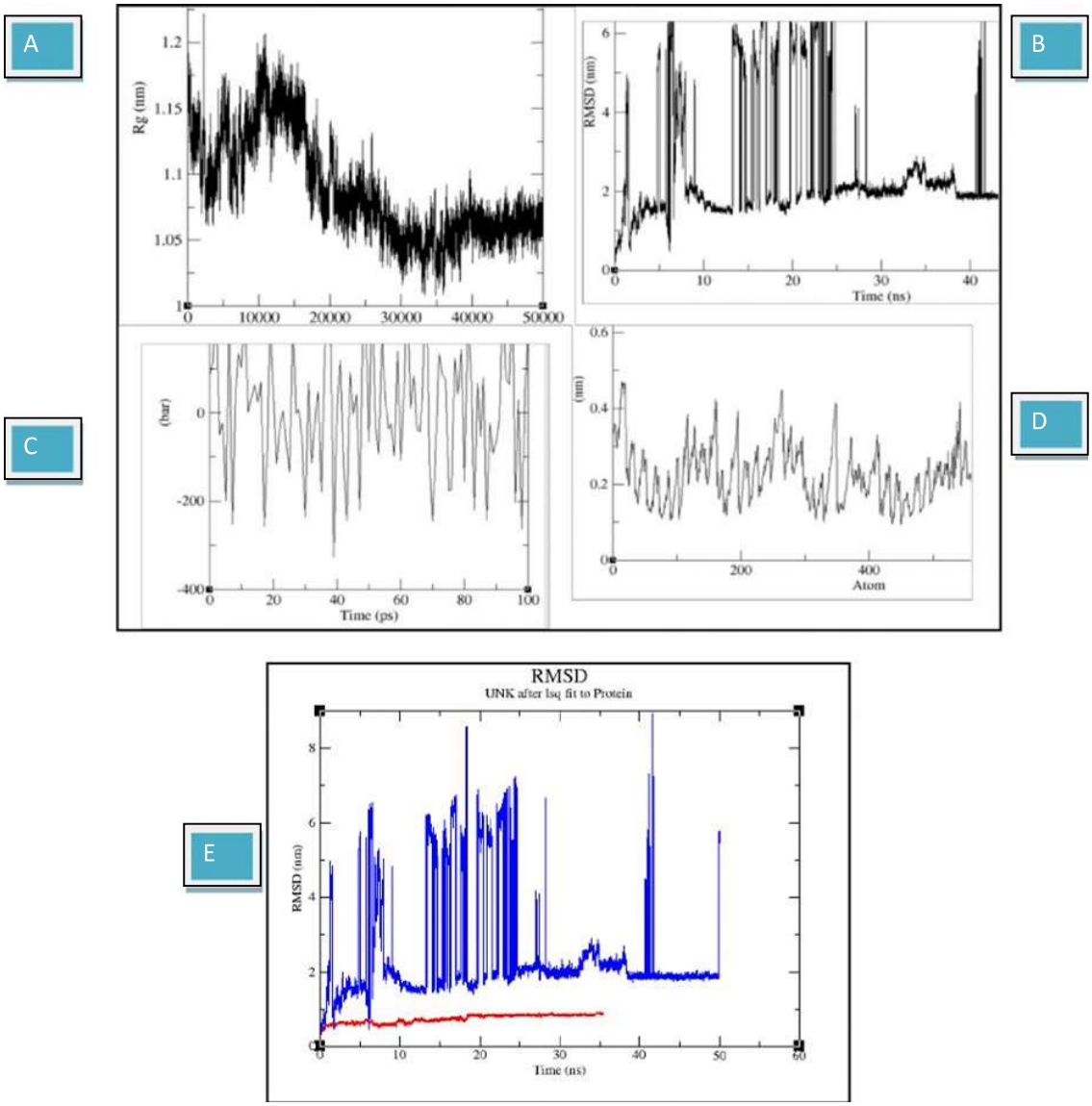

Figure 5.3. Simulation graphs showing (A) radius of gyration (B) rmsd (root mean square density) of modified gedunin $C_{26}H_{31}N_2O_6F$ (C) pressure (D) rmsf (root mean square fluctuations) (E) RMSD of the complex where blue represents modified gedunin $C_{26}H_{31}N_2O_6F$, and red represents 5‟‟nt enzyme.

The overall simulation analysis shows that the molecule binds to the active centre of 5'NT, and the complex becomes stable **(Figure 5.3.).** Ramachandran plot analysis of all complex residues and analysis by the Prove server with a mean z-

score of 0.931**.**The higher the z-score, the more stable the complex**(Dagar *et al.*, 2021).**

5.3.3. ADME

Drug absorption through the GI tract is measured by human intestinal absorption (HIA), which is responsible for the oral administration of the drug. The total absorbed mass/dose of the drug is shown in **Table 5.6**. Lipinski's Rule of Five determines the biological activity of a drug. The Lipinski rule has a molecular weight < 500 Dalton, log P <5: it is a measure of the lipophilicity of a compound that has many physiological properties such as metabolic rate, binding site interaction, hydrogen bond acceptor (HBA) <10, and hydrogen bond donor can affect (HBD) <5, whereby all these properties are replaced by some physical properties such as TPSA, log S> 2: it is responsible for the intrinsic solubility of the molecule, and it is crucial for the formulation of each drug molecule; log D: it is for lipophilicity at relevant pH and is better suited to predict the biological activity of the compound **(Pai *et al.*, 2016).**

Drug distribution via the blood makes up the BBB category <0.5. it is the ability of the drug to penetrate the barrier and is essential in the case of CNS targets, while drugs with non-CNS targets with barrier penetration are undesirable. **Table 5.6.** shows that the ligand is a non-CNS drug. This was further shown in SwissADME and medicinal chemistry analyses.

Substance pharmacokinetics, medicine chemical treatment, and drug probability were assessed using SwissADME, a web-based online server. The Swiss ADME tool is built upon the Vector Machine Algorithm concept, which allows rapid analysis of the data sets of known non-inhibitors and substrates.

TPSA is a topological polar surface representing the molecule's hydrogen bonding capacity and GI absorption (less than 140 A ^ two good absorption), which determines the blood-brain barrier (less than 90 A ^ 2 Permeable). Lipophilicity (XLOGP3) is represented by log P, which is suitable for oral bioavailability in the range of 1-3. The solubility (log S) was in the range of 1–6. The molecular weight and rotational bonds of no more than nine are good for flexibility. The druggness of the molecule is defined using the Lipinski filter, Veber filter, Ghosh filter, Egan filter, and Muegge filter **(Pai et *al.,* 2016).**

The medicinal chemistry region enables the identification of potentially problematic fragments. This part has Pain Warning; Pain is the molecules containing some substructures that show a strong response (false positive output) in assays regardless of the protein target. If a molecule contains such units, SwissADME returns a warning. The Brenk filters in SwissADME return warning messages if reactive, toxic, and metabolically unstable fragments are present. It was observed that ligand has higher hydrophobicity and size of> 300 and other favourable factors, which makes it suitable as a "lead" in the lead process optimization process.

Boiled eggs help to assess the blood-brain barrier (BBB) and gastrointestinal (GI) absorption. **Figure 5.4** shows a boiled egg diagram, with the yellow (egg yolk) region indicating the likelihood of brain penetration and the white region indicating passive absorption through the gastrointestinal tract. Molecules can have blue or red colors for P-gp (+) or P-gp (-). Blue: emanated from P-gp (PGP +), and red: non-substrate of P-gp (PGP). The ligand marked as a blue dot is predicted to be PGP + (P-gp substrate) but does not reach the brain (in white) and

is not absorbed by the GI (in yellow) because it is outside the diagram area. Further toxicity and metabolism were analyzed using the stardrop software.

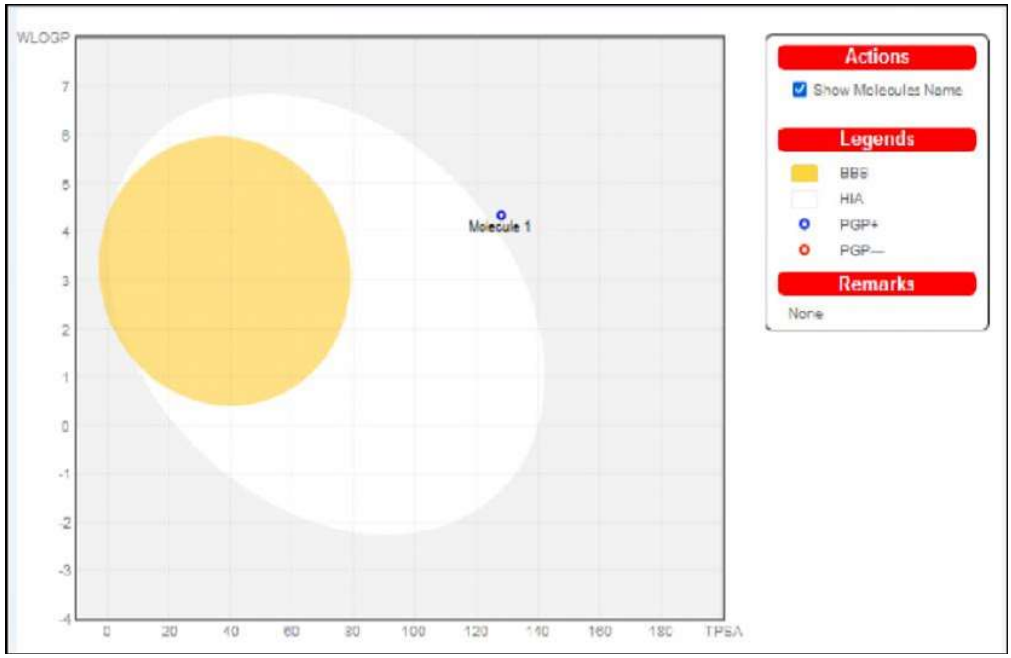

Figure 5.4 Boiled – egg representation of molecule $C_{26}H_{31}N_2O_6F$. The white region represents passive absorbtion by the GI tract; the yellow region depicts brain penetration probability. The grey region is non-BBB permeant and has low GI absorption.

Metabolism is a chemical modification of a drug that increases its solubility and hydrophobicity for excretion. Seven drugs metabolize the isoform of P450, namely CYP2D6, CYP2C19, CYP2C9, CYP3A4, CYP1A2, CYP2C8, and CYP2E1 while **Table 5.5.** shows that the ligand has broad substrate specificity, primarily through the phase 1 enzyme CYP Isoform 3A4 with a probability of 0.9691. It metabolizes drug-consuming oxidation, hydrolysis, and reduction reactions and is present in the liver, gastrointestinal tract, brain, lungs, placenta, and kidneys. The cytochrome P450 metabolism model predicted by the Stardrop software has three main outputs:

1. P450 predicts which isoform of the seven cytochrome P450s would significantly metabolize a compound. **Table 5.5.** shows a probability of 0.66 according to isoform 3A4.
2. Regioselectivity provides information on the most likely metabolites formed when a molecule is a substrate for one isoform. The metabolism landscape is shown in **Figure 5.7.** shows the regioselectivity of the ligand for isoform 3A4.
3. Localization labiality is a measure of metabolism efficiency at this position. **Figure 5.5.** shows that C25 and C27 are more labile than the other ligand sites.

Inhibition of 2C9_Pki and hERG pic50, shown in **Table 5.8.,** should not be present to avoid drug interactions. 2C9_Pki <6 predicts the Pki values for CYP2C9 isoform affinity of P450 cytochrome. hERG pic50 <6.3 is the Inhibition of the potassium channel-related gene (hERG) responsible for a prolonged QT interval, which leads to ventricular arrhythmias. The ligand showed no inhibition of 2C9_Pki and hERG pic50, as shown in **Table 5.6,** using Star-Drop software.

Table 5.5 P450 Isoform Classification of Inhibitor ($C_{26}H_{31}N_2O_6F$)

	Isoform Type	Probability value
Majorly belongs to3A4 Isoform	1A2	0.024
	2C19	0.062
	2C8	0.096
	2C9	0.11
	2D6	0.034
	2E1	0.006
	3A4	0.668
P450_3A4_Sites	C1 2.65034e-5 stable C3 1.68453e-6 stable C4 1.28204e-6 stable C5 7.96064e-7 stable C12 2.7001e-5 stable C13 7.07775e-7 stable C14 6.99382e-7 stable C17 7.58538e-8 stable C22 0.000948583 stable C24 0.000201541 stable C25 96.0074 labile C27 3.98283 mod labile C28 1.85384e-6 stable C33 0.00156411 stable C35 5.51779e-5 stable C7=C8 0.00692835 stable	
P450_3A4_CSL	0.9691	
P450_3A4_CSL_Uncertainty	0.04868	

	form Type	Probability value
Majorly belongs to3A4 Isoform		
	2C19	0.062
	2C8	0.096
	2C9	0.11
	2D6	0.034
	2E1	0.006
	3A4	0.668
P450_3A4_Sites	C1 2.65034e-5 stable	
P450_3A4_CSL	0.9691	
P450_3A4_CSL_Uncertainty	0.04868	

Table 5.6. ADME Properties: Probability scoring profile of inhibitor

5 7.96064e stable

($C_{26}H_{31}N_2O_6F$). (a) the inhibitor is Non - CNS, and non-BBB permeable and has a C12 7001e 5 t bl

low score for 2C9_pKi.(b) inhibitor is not an inhibitor of p-gp with the most negligible probability score.

(a)

Profile Name	ScoreC	Standard 00094858 Deviation	e Desired value (According to ble Lipinski's rule of five)
Intravenous CNS Scoring Profile Score	C24 0.07932	000201 0.1037	ble NA
Intravenous Non-CNS Scoring Profile Score	0.1906	0.1894	NA
Lipinski Rule of Five Score	1	85.384e-6 0.000846	e NA
Oral CNS Scoring Profile Score	C33 0.04286	0015640.0828[1]	le NA

Oral Non-CNS Scoring Profile Score	0.103	0.1619	NA
BBB log brain blood	-0.8012	Inf	-0.2 to 1
Log S	0.1163	1.033	>2
logS_pH7_4	0.1163	1.033	NA
Log P	2.831	0.4351	0 -3
Log D	2.831	0.4351	0 -3
2C9_pKi	5.304	Inf	<6
hERG_pIC50	4.193	0.9567	<6.3
Mol .weight	486.5	0	<500 DA
HBD	2	0	0 – 5
HBA	8	0	0 – 10
TPSA	128.1	0	<140 A^2
Flexibility	0.075	0	NA
Rotatable bonds	3	0	0 -9

(b)

Property	Category	Probability	Desired value
BBB category	-	0.74	-
HIA category	+	0.863636	+
P _gp Inhibitor	No	0.53	NO
2D6_affinity_category	Very high	0.5625	<6
PPB90_category	Low	0.58	Low

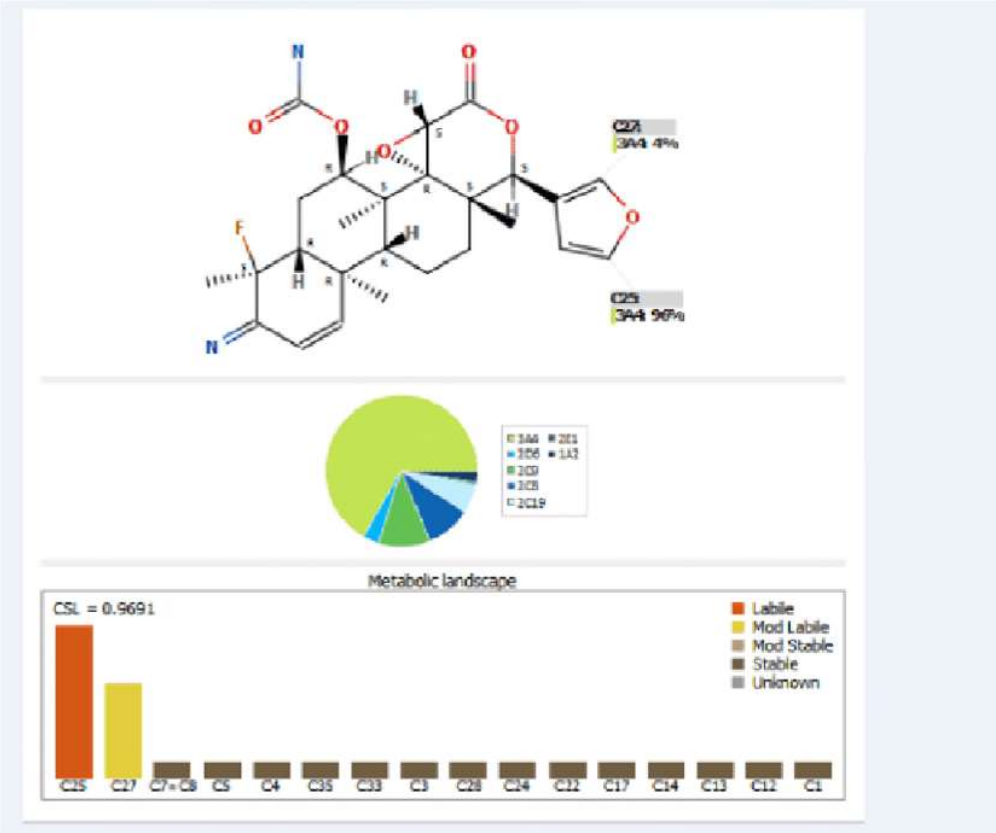

Figure 5.5. P450 Isoform type for substrate inhibitor $C_{26}H_{31}N_2O_6F$ is Majorly 3A4 (the green region in the pie chart). The red bar in the metabolic landscape represents the most liable (96%)component of the inhibitor, i.e. C25 by 3A4 decomposition. The yellow bar represents C27 as a moderate liability (4%).

5.3.4. Toxicity

The Derek Nexus tool was used to calculate toxicity risk based on the structural features of the molecule. It is a knowledge-based toxicity prediction tool developed by Lhasa Limited and available on the Stardrop platform **(Zou *et al.*, 2020).** A toxicity report indicates the likelihood, such as:

No report is an endpoint, and there is no reason to raise an alert or predict inactivity or activity based on the molecule's physical properties. Equivocal is sufficient and equal evidence for or against a statement. Evidence supports this

statement. Plausible, this is the case when there is no argument against the statement with at least one valid reason.

The ligand in **Table 5.7.** shows the Derek nexus probability, so there is an equivocal report on carcinogenicity, while it is plausible for skin sensitization, developmental toxicity, hepatotoxicity, skin irritation, and eye irritation. The oral toxicity prediction is shown in **Figure 5.6.** was from Protox II, the LD50 was 274 mg/kg, and the ligand fell into toxicity class three of the compounds.

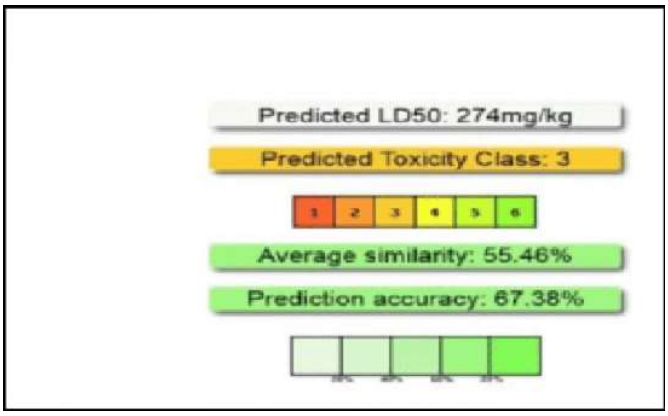

Figure 5.6. Oral toxicity prediction of $C_{26}H_{31}N_2O_6F$.

Table 5.7. Toxicity prediction profiling of inhibitor $C_{26}H_{31}N_2O_6F$ using Derek-Nexus Likelihood in Stardrop. Plausible reports suggest that the inhibitor can cause skin and eye irritation. The carcinogenicity profile is equivocal of proposition for and against of inhibitor.

PROPERTY	REPORT
Photo – allergenicity	No Report
Occupational asthma	No Report
Respiratory sensitization	No Report
Splenotoxicity	No Report
Teratogencity Probability	No Report
Testicular toxicity	No Report
Adrenal gland toxicity	No Report

Thyroid toxicity	No Report
Ocular toxicity	No Report
Pulmonary toxicity	No Report
Skin sensitization	Plausible
Developmental toxicity	Plausible
Hepatotoxicity	Plausible
Skin irritation	Plausible
Eye irritation	Plausible
Carcinogenicity	Equivocal

The toxicity of a drug is due to the groups present in the drug. Bioactivity was identified for the R groups and their roles in ADME properties and biosteres **(Zaretzki *et al.*, 2012)** for the ligand. These are synthetically and chemically validated databases of 29,012 compound pairs that have been compiled and cover a wide range of chemical conversions. Biosters are chemical groups with similar chemical and physical properties and have somewhat similar biological properties. If biosters are responsible for the toxicity in one compound, replacing this bioster with another will give the desired properties without changing the structure of the compound **(Daina *et al.*, 2017).** A new chemical/molecule has similar biological characteristics to the parent compound. The primary objective of any bio-isosteric substitution or bioisosteric replacement is to reduce toxicity and modify molecular pharmacokinetics. **Figure 5.7.** shows the ligand's bioactivity of the R groups using the luminous molecular properties of the Stardrop Software. The blue color shows a decrease in bioactivity, the green color shows no effect, and the red color shows an increase in the bioactivity of the group, resulting in an overall change in drug/ligand bioactivity. In the BBB log, nitrogen substitution decreases the predictive value for blood-brain barrier permeability, whereas carcinogenicity,

alteration of the inhibitor, has no effect. Changes in developmental toxicity do not affect the value of developmental toxicity. Changes in eye irritation do not affect the plausible toxicity reports of eye irritation.

Skin irritation changes did not affect the toxicity reports of skin irritation. HBA modification increased the number of hydrogen bond acceptors of the inhibitor according to the Lipinski definition, whereas HBD modification increased the number of hydrogen bond donors according to the Lipinski definition. Log P modification decreased log P. Log S modification value did not affect log S of the inhibitor. Log D change decreased the value of Log D., while TPSA change increased the value of TPSA. Intra, CNS modifications decrease the probability of CNS penetration, whereas intra- and non-CNS modifications make molecules non-CNS. No effect was observed in the oral CNS. In the oral cavity, non-CNS modification decreased the oral non-CNS profile score of the inhibitor.

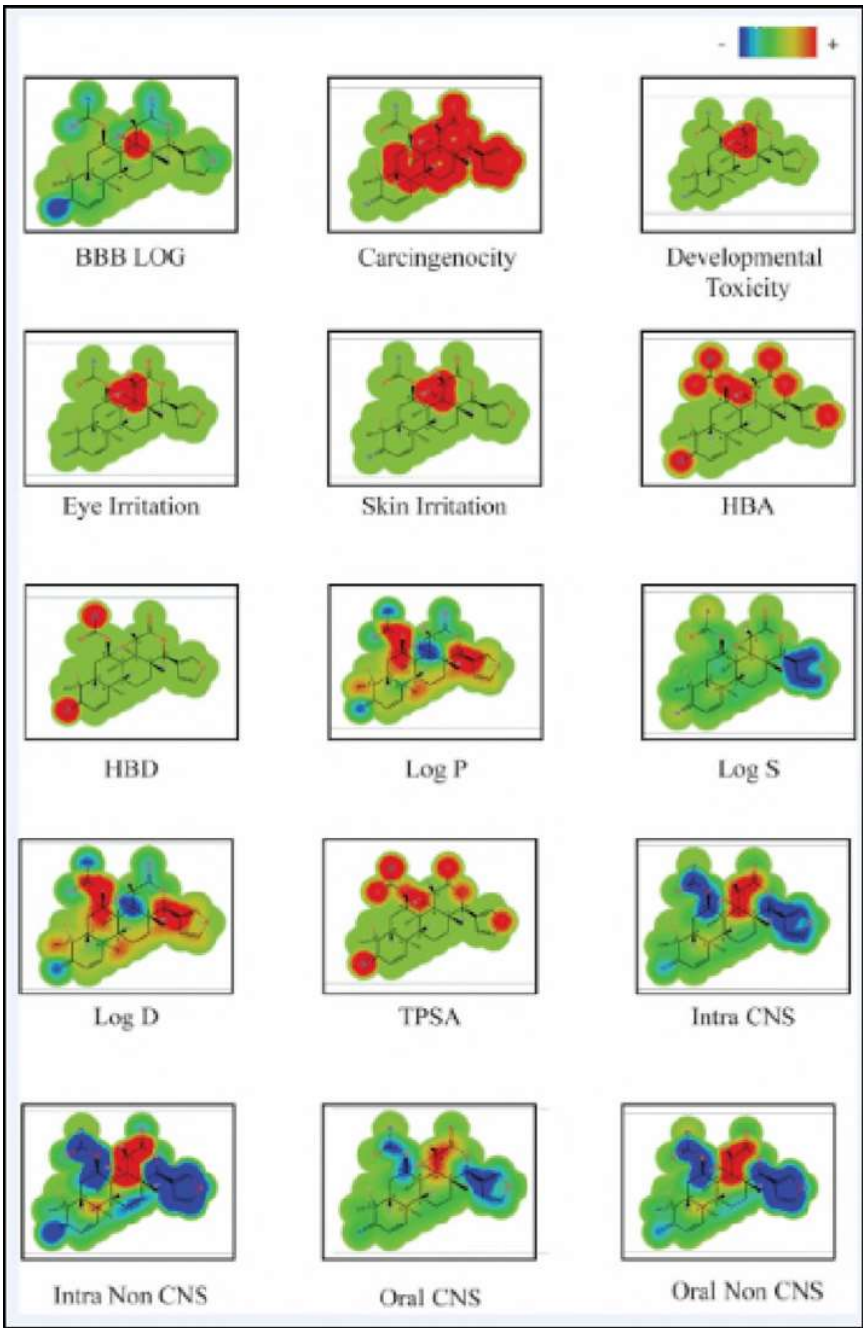

Figure 5.7. Biostere: Glowing molecule visualization of ADMET + DEREK NEXUS LIKLIHOOD properties of the inhibitor $C_{26}H_{31}N_2O_6F$. The red region is increasing the predicted value; the blue region is decreasing the predicted value, whereas the green region does not affect.

5.3. Conclusion

An inhibitor $C_{26}H_{31}N_2O_6F$ molecular docking study demonstrated the ability of the molecule to act as an inhibitor of snake venom enzymes with improved pharmacokinetic, physicochemical, and drug-like properties. The inhibitor is a non-cns intravenous drug that does not cross the blood-brain barrier, and it is an oral non-cns drug with molecular weight, polarity, and Hydrophobicity that comes under the Lipinski rule of 5. The synthesized compound could be used as a therapeutic agent against snake venom.